Multiband k·p models for strained zincblende crystals: Application to the fine structure of ZnO

F. Michelini,* N. Cavassilas, R. Hayn, and M. Szczap
IM2NP, Aix-Marseille Université, Bâtiment IRPHE, Technopôle Château-Gombert, F-13384 Marseille Cedex 13, France
(Received 27 February 2008; revised manuscript received 8 October 2009; published 15 December 2009)

The elementary-matrix blocks of multiband k·p models are derived for strained zincblende crystals using methods of group theory. The general viewpoint we adopted is exploited in two opposite directions: the global description of the first Brillouin zone and the fine structure of the valence-band maximum. First, full-zone models are completed: strain contributions originating from the orbital and spin-orbit parts of the Hamiltonian are included in the 30-band model while the next 54-band model is introduced. Second, a 16-band spin-orbit Hamiltonian is constructed for ZnO with zincblende-type structure. The reversed level order at the valence-band maximum is attributed to the T_2-T_2 *pd -like* coupling actually taken into account. We perform *ab initio* calculations in the local-density approximation including relativistic effects to estimate the coupling parameter ζ_{12}=250 meV that gives an amount of *pd*-like interband mixing of about 10%.

DOI: 10.1103/PhysRevB.80.245210 PACS number(s): 71.15.Ap, 71.20.Nr, 71.70.Ej

I. INTRODUCTION

Semiconductor-based mesoscopic structures are over running the technology of electronics and optoelectronics, and hence hold more and more attention from fundamental viewpoints. In the frontier in between microscopic descriptions and microelectronics, new k·p models are expected to provide suited and comprehensible descriptions for emerging new kinds of quantum systems. Different improvements of modeling can be proposed in the framework of the k·p method. Let us distinguish three of the main directions. (i) The number of bands increases to describe larger (E,k) regions of the first Brillouin zone. Such a perspective leads to the ultimate full-zone models.[1–4] (ii) New bands are added to describe the impacts of interband couplings. The eight-band model[5,6] is still widely used to investigate interactions between the conduction band and the valence band. Nonparabolicity and warping in the conduction band of GaAs were addressed by considering the coupling between the valence band and the second conduction band in a 14-band model.[7] Besides, the eight-band model was recently extended toward a ten-band k·p model for diluted nitride alloys of III-V semiconductors.[8] A *s -like* higher-lying band formed by nitrogen resonant states was added to account for the dramatic changes in Ga(N)As electronic structures. (iii) Still ignored terms of the effective Hamiltonian are taken into account in a given model. The linear k terms that arise from the spin-orbit part of the Hamiltonian were introduced by Dresselhaus[9] in the four-band model for the valence band of zincblende structures. Bir and Pikus[10] derived the strain-induced terms in the framework of the k·p theory, and treated some of these terms in the spinless three-band model for the valence band. To advance forthcoming investigations in the mesoscopic physics of electrons, it seems urgent to adopt a general viewpoint on the k·p method.

The present paper provides in compact form the elementary coupling blocks needed to construct multiband k·p models for strained zincblende crystals. We use them to provide new developments within the k·p method. In full-zone modeling, ignored interactions as well as remote bands are now taken into account. In point-zone modeling, a 16-band spin-orbit Hamiltonian is achieved for the ZnO valence band.

In the first part (Sec. II), we give all the matrix blocks entering k·p models. A model is representing the effective Hamiltonian for an electron in a strained zincblende structure. We use the most general form of that operator taking into account spin orbit as strain contributions. The operator coupling terms and their origins are recalled in Sec. II A. The main issue of this part is developed in Sec. II B. We consider all the possible electronic states at the Γ point, which boils down to consider all the possible state symmetries only. Indeed, methods of group theory are used to derive all the coupling terms in matrix form, between the five (respectively, ten in O_h) irreducible representations of the T_d symmetry group. Second part is dedicated to models. The first type (Sec. III A) is defined as full-zone models for which a high number of bands is required to describe the significant effects of strain, confinement, or external excitation on the whole Brillouin zone. The existing 30-band model is completed by including the strain interactions originating from the orbital and the spin-orbit parts of the Hamiltonian [point (iii)]. Furthermore the next higher level 54-band model that involves a new irreducible representation in the O_h symmetry group is introduced [points (i) and (ii)]. The second type of models (Sec. III B) deals with the valence band of II-VI semiconductors for which the lower-lying "metal" *d*-like bands strongly influence the fine structure of the valence-band maximum. That ten bands are added to the standard valence-band basis to derive the spin-orbit Hamiltonian at the Γ point. The 16-band model we constructed allows to account for the dramatic impacts of the *pd*-like spin-orbit coupling at the valence-band maximum[11,12] [point (ii)]. Focus is put on the inversion of the spin-orbit splitting in ZnO, which is of high importance both for spintronics and for optoelectronics.[13] The empirical spin-orbit parameter and interband mixing proportion are extracted from fit on *ab initio* results obtained in the local-density approximation.

All group theory informations are taken from the complete book of Altmann and Herzig[14] and a dictionary of different systems of notations for the irreducible representations of point groups is given in Table I with respect to the widely used reference book of Koster *et al.*[15] In the O_h symmetry

TABLE I. Dictionary of all the irreducible representations in the cubic groups T_d and O_h. From left to right: notations used from Ref. 15 for the T_d symmetry group. Spin is included by forming the direct product with the representation of the spin function, Γ_6 in Ref. 15. The decomposition in double group irreducible representations is thus given. Notations from Ref. 14 for the T_d symmetry group and Cartesian tensors and basis functions ($\omega^3=1$) for the irreducible representations of the simple group (**R** represents an axial vector). The spin function transforms according to the representation $E_{1/2}$. Notations from Ref. 14 for the O_h symmetry group and basis functions for the split representations.

T_d (Ref. 15)	$\Gamma\times\Gamma_6$	T_d (Ref. 14)		$\Gamma\times E_{1/2}$	O_h (Ref. 14)		
Γ_1	Γ_6	A_1	$a_1=1$	$E_{1/2}$	A_{1g}	A_{2u}	xyz
Γ_2	Γ_7	A_2	a_2	$E_{5/2}$	A_{2g}	A_{1u}	
Γ_3	Γ_8	E	$\begin{cases} e_1=\omega^* x^2+\omega y^2+z^2 \\ e_2=\omega x^2+\omega^* y^2+z^2 \end{cases}$	$F_{3/2}$	E_g	E_u	$\begin{cases} ixyze_1 \\ -ixyze_2 \end{cases}$
Γ_4	Γ_6,Γ_8	T_1	R_x,R_y,R_z $x(y^2-z^2),y(z^2-x^2),z(x^2-y^2)$	$E_{1/2},F_{3/2}$	T_{1g}	T_{2u}	
Γ_5	Γ_7,Γ_8	T_2	x,y,z	$E_{5/2},F_{3/2}$	T_{1u}	T_{2g}	iyz,izx,ixy

group, each representation splits into an even [subscript g (Ref. 14) and superscript + (Ref. 15)] and an odd (subscript u and superscript −) representations with the additional inversion operation.

II. MULTIBAND k·p COUPLINGS

A. Theoretical framework

The operator $\mathcal{H}$ representing the band-structure changes induced by a homogeneous strain was derived by Bir and Pikus[10] starting from the Hamiltonian of an electron in a strained crystal

$$H=\frac{\mathrm{p}^2}{2m_0}+V_{\boldsymbol{\epsilon}}+\frac{\hbar}{4m_0^2c^2}[\nabla V_{\boldsymbol{\epsilon}},\mathrm{p}]\cdot\boldsymbol{\sigma}, \tag{1}$$

where $\boldsymbol{\epsilon}=[\epsilon_{\alpha\beta}=\frac{1}{2}(\frac{du_\alpha}{dx_\beta}+\frac{du_\beta}{dx_\alpha})]$ is the symmetric strain tensor that defines the applied strain, $u(\mathbf{x})$ is the vector displacement, where $V_{\boldsymbol{\epsilon}}$ is the periodic potential in the strained crystal and $\boldsymbol{\sigma}=(\sigma_x,\sigma_y,\sigma_z)$ are the Pauli spin matrices. Such a problem cannot be solved using a perturbation approach nor direct symmetry analysis of the strained structure. To circumvent these difficulties, the system is subjected to a coordinate transformation making the positions of the Bravais lattice points in the new coordinate system coincide with their positions in the unstrained lattice in the old coordinate system. That transformation yields the new operator

$$H=H_0+H_{\boldsymbol{\epsilon}}+H_{\boldsymbol{\epsilon}\mathrm{so}}, \tag{2}$$

where

$$H_0=\frac{\mathrm{p}^2}{2m_0}+V_0+H_{\mathrm{so}} \tag{3a}$$

with

$$H_{\mathrm{so}}=\frac{\hbar}{4m_0^2c^2}[\nabla V_0,\mathrm{p}]\cdot\boldsymbol{\sigma} \tag{3b}$$

$$H_{\boldsymbol{\epsilon}}=-\frac{\mathrm{p}\boldsymbol{\epsilon}\mathrm{p}}{m_0}+\mathbf{V}\boldsymbol{\epsilon}, \tag{3c}$$

$$H_{\boldsymbol{\epsilon}\mathrm{so}}=\frac{\hbar}{4m_0c^2}\{[\nabla\mathbf{V}\boldsymbol{\epsilon},\mathrm{p}]\cdot\boldsymbol{\sigma}-[\boldsymbol{\epsilon}\nabla V_0,\mathrm{p}]\cdot\boldsymbol{\sigma}-[\nabla V_0,\boldsymbol{\epsilon}\mathrm{p}]\cdot\boldsymbol{\sigma}\}, \tag{3d}$$

where V_0 is the periodic potential of the unstrained crystal. The operator H_0 is the Hamiltonian of an electron in the unstrained crystal, where $V_{\boldsymbol{\epsilon}}$ has been merely replaced by V_0. The components of $\mathbf{V}$ read

$$V_{\alpha\beta}(\mathbf{x})=\frac{1}{2-\delta_{\alpha\beta}}\lim_{\boldsymbol{\epsilon}\to 0}\frac{V_{\boldsymbol{\epsilon}}[(1+\boldsymbol{\epsilon})\mathbf{x}]-V_0(\mathbf{x})}{\epsilon_{\alpha\beta}}.$$

Fo1lowing the k·p procedure, the Bloch theorem is exploited to form the effective operator $\mathcal{H}$ that determines the energies and the envelopes of the Bloch functions. In the strained crystal, $\mathcal{H}$ reads

$$\mathcal{H}=\mathcal{H}_0+\mathcal{H}_{\mathbf{K}_{\boldsymbol{\epsilon}}\cdot\mathbf{p}}+\mathcal{H}_{\boldsymbol{\epsilon}}+\mathcal{H}_{\mathrm{kso}}+\mathcal{H}'_{\boldsymbol{\epsilon}\mathrm{so}}, \tag{4}$$

where

$$\mathcal{H}_0=\frac{\mathrm{p}^2}{2m_0}+V_0+\frac{\hbar^2k^2}{2m_0}, \tag{5a}$$

$$\mathcal{H}_{\mathbf{K}_{\boldsymbol{\epsilon}}\cdot\mathrm{p}}=\frac{\hbar}{m_0}\mathrm{p}\cdot\mathbf{K}_{\boldsymbol{\epsilon}}, \tag{5b}$$

$$\mathcal{H}_{\boldsymbol{\epsilon}}=H_{\boldsymbol{\epsilon}}, \tag{5c}$$

$$\mathcal{H}_{\mathrm{kso}}=\frac{\hbar^2}{4m_0^2c^2}[\boldsymbol{\sigma},\nabla V_0]\cdot\mathrm{k}, \tag{5d}$$

$$\mathcal{H}'_{\boldsymbol{\epsilon}\mathrm{so}}=H_{\mathrm{so}}+H_{\boldsymbol{\epsilon}\mathrm{so}} \tag{5e}$$

with $\mathbf{K}_{\boldsymbol{\epsilon}}=(1-\boldsymbol{\epsilon})\mathrm{k}$ and $\mathcal{H}_{\boldsymbol{\epsilon}}\equiv H_{\boldsymbol{\epsilon}}$.

In the framework of the k·p method, the operator $\mathcal{H}$ is projected on a finite Bloch basis at the Γ point. A group of bands is selected to describe the electronic properties of the system as it will be illustrated in Sec. III. The aim in this part is to provide all the coupling matrix blocks that are necessary

TABLE II. Matrix blocks of the different terms of the operator $\mathcal{H}$ [see Eq. (4)]. Each block represents a nonzero matrix coupling between two Bloch states at the Γ point. The block form depends only on the state symmetries (see Table III). The notation for the blocks (calligraphic letters $\mathcal{P}$) is similar to the notation for the corresponding scalar parameters (roman letters P, Greek letters are used when spin is included).

	Matrix coupling blocks
$\mathcal{H}_0$	$\mathcal{I}$
$\mathcal{H}_{\mathbf{K}_\epsilon \cdot \mathrm{p}}$	$\mathcal{P},\mathcal{Q},\tilde{\mathcal{Q}},\mathcal{R},\tilde{\mathcal{R}}$
	$\mathcal{A}$
$\mathcal{H}_\epsilon$	$\mathcal{B},\tilde{\mathcal{B}},\mathcal{E},\mathcal{D}$
	$\mathcal{C},\mathcal{F},\tilde{\mathcal{F}},\mathcal{G},\tilde{\mathcal{G}}$
$\mathcal{H}_{\mathrm{kso}}$	$\mathcal{X},\mathcal{Y},\tilde{\mathcal{Y}},\mathcal{Z},\tilde{\mathcal{Z}}$
$\mathcal{H}'_{\epsilon\mathrm{so}}$	$\mathcal{S},\tilde{\mathcal{S}},\mathcal{T},\tilde{\mathcal{T}},\mathcal{U}$

to form any matrix representing the operator $\mathcal{H}$ on the chosen restriction.

B. Couplings blocks

Tables II and III provide the elementary material to form any $\mathcal{H}$ matrix representation from symmetry considerations only.[16] For a given term of $\mathcal{H}$ in Table II, each matrix block represents one of the nonzero couplings between two types of function symmetry at the Γ point. State symmetries are identified by the irreducible representations according which states transform. They are used in the double entry Table III. The $\mathcal{H}$ matrix coupling between two bands is a linear combination of all the matrix blocks listed in Table III. A coefficient represents a *scalar parameter* to be estimated from fitting procedures with experimental measurements and/or *ab initio* calculations. Block forms follow.[17]

The operator $\mathcal{H}_0$ [Eq. (5a)] transforms such as A_1 in the T_d symmetry group (A_{1g} in O_h). The coupling $\mathcal{I}$ occurs inside the same level only. The block is proportional to the identity matrix of the representation dimension with the coefficient

$$I = E + \frac{\hbar^2 k^2}{2m_0}. \tag{6}$$

The operator p transforms such as T_2 in the T_d symmetry group (T_{1u} in O_h). The blocks $\mathcal{P},\mathcal{Q},\mathcal{R}$ and $\tilde{\mathcal{Q}},\tilde{\mathcal{R}}$ representing $\mathcal{H}_{\mathbf{K}_\epsilon \cdot \mathbf{p}}$ [Eq. (5b)] have the forms

$$\mathcal{P} = P(K_{\epsilon_x} \;\; K_{\epsilon_y} \;\; K_{\epsilon_z}), \tag{7a}$$

$$\mathcal{Q} = Q\begin{pmatrix} 0 & K_{\epsilon_z} & K_{\epsilon_y} \\ K_{\epsilon_z} & 0 & K_{\epsilon_x} \\ K_{\epsilon_y} & K_{\epsilon_x} & 0 \end{pmatrix}, \tag{7b}$$

$$\tilde{\mathcal{Q}} = \tilde{Q}\begin{pmatrix} 0 & -iK_{\epsilon_z} & iK_{\epsilon_y} \\ iK_{\epsilon_z} & 0 & -iK_{\epsilon_x} \\ -iK_{\epsilon_y} & iK_{\epsilon_x} & 0 \end{pmatrix},$$

TABLE III. Nonzero coupling blocks between the irreducible representations according which states transform at the Γ point in the T_d and O_h symmetry groups. The trivial block $\mathcal{I}$ have been omitted. In O_h, one has to apply the additional parity rule involving the u,g characters of the operator and the two states in order to identify the vanishing coefficients (obtained when a odd number of times u occurs, like in the gug product).

T_d	A_1	A_2	E		T_1			T_2	
A_1				$\mathcal{U}$				$\mathcal{X}$	$\mathcal{P}$
	$\mathcal{A}$			$\mathcal{B}$					$\mathcal{C}$
A_2					$\mathcal{X}$	$\mathcal{P}$	$\mathcal{U}$		
		$\mathcal{A}$		$\tilde{\mathcal{B}}$		$\mathcal{C}$			
E				$\mathcal{T}$	$\tilde{\mathcal{Z}}$	$\tilde{\mathcal{R}}$	$\tilde{\mathcal{T}}$	$\mathcal{Z}$	$\mathcal{R}$
			$\mathcal{A}$	$\mathcal{E}$		$\tilde{\mathcal{F}}$			$\mathcal{F}$
T_1				$\mathcal{S}$	$\mathcal{Y}$	$\mathcal{Q}$	$\tilde{\mathcal{S}}$	$\tilde{\mathcal{Y}}$	$\tilde{\mathcal{Q}}$
				$\mathcal{A}$	$\mathcal{D}$	$\mathcal{G}$		$\tilde{\mathcal{D}}$	$\tilde{\mathcal{G}}$
T_2							$\mathcal{S}$	$\mathcal{Y}$	$\mathcal{Q}$
							$\mathcal{A}$	$\mathcal{D}$	$\mathcal{G}$

O_h	A_1	A_2	E		T_1			T_2	
A_1				$\mathcal{U}$	$\mathcal{X}$	$\mathcal{P}$			
	$\mathcal{A}$			$\mathcal{B}$					$\mathcal{C}$
A_2							$\mathcal{U}$	$\mathcal{X}$	$\mathcal{P}$
		$\mathcal{A}$		$\tilde{\mathcal{B}}$		$\mathcal{C}$			
E				$\mathcal{T}$	$\mathcal{Z}$	$\mathcal{R}$	$\tilde{\mathcal{T}}$	$\tilde{\mathcal{Z}}$	$\tilde{\mathcal{R}}$
			$\mathcal{A}$	$\mathcal{E}$		$\tilde{\mathcal{F}}$			$\mathcal{F}$
T_1				$\mathcal{S}$	$\tilde{\mathcal{Y}}$	$\tilde{\mathcal{Q}}$	$\tilde{\mathcal{S}}$	$\mathcal{Y}$	$\mathcal{Q}$
				$\mathcal{A}$	$\mathcal{D}$	$\mathcal{G}$		$\tilde{\mathcal{D}}$	$\tilde{\mathcal{G}}$
T_2							$\mathcal{S}$	$\tilde{\mathcal{Y}}$	$\tilde{\mathcal{Q}}$
							$\mathcal{A}$	$\mathcal{D}$	$\mathcal{G}$

$$\mathcal{R}(\tilde{\mathcal{R}}) = R(\tilde{R})\begin{pmatrix} \omega K_{\epsilon_x} & \omega^* K_{\epsilon_y} & K_{\epsilon_z} \\ s\text{-}\omega^* K_{\epsilon_x} & s\text{-}\omega K_{\epsilon_y} & s\text{-}K_{\epsilon_z} \end{pmatrix} \tag{7c}$$

with $\omega = \exp(i\frac{2\pi}{3})$ and $s\text{-} = -1$ for tilde block $\tilde{\mathcal{R}}$, 1 otherwise. The bases shown in Table I may be selected for the irreducible representations. All $\{P,Q,R\}$ and $\{\tilde{Q},\tilde{R}\}$ are scalar parameters to be estimated. All of them contribute to both strained and unstrained structure descriptions. Besides, it has been shown[9] that Q vanishes inside a same degenerate level. In the unstrained case, the well-known Kane parameter P is recovered between the conduction and the valence bands[5] as the parameter Q between the second conduction band and the valence band.[7]

As the components of $\boldsymbol{\epsilon}$, components of $\mathbf{V}$ and products $p_i p_j$ transform according to the same representation that decomposes into the irreducible representations A_1, E, and T_2 in the T_d symmetry group (A_{1g}, E_g, and T_{2g} in O_h). The strain tensor is here written according to its standard components ($\omega^3 = 1$)

$$\begin{cases} \epsilon_1 = \epsilon_{xx} + \epsilon_{yy} + \epsilon_{zz} \\ \epsilon_2 = \omega^* \epsilon_{xx} + \omega \epsilon_{yy} + \epsilon_{zz} \\ \epsilon_3 = \omega \epsilon_{xx} + \omega^* \epsilon_{yy} + \epsilon_{zz} \\ \epsilon_4 = \epsilon_{yz} \\ \epsilon_5 = \epsilon_{zx} \\ \epsilon_6 = \epsilon_{xy} \end{cases}. \tag{8}$$

The blocks $\mathcal{A},\mathcal{B},\mathcal{C},\mathcal{D},\mathcal{E},\mathcal{F},\mathcal{G}$ and $\tilde{\mathcal{B}},\tilde{\mathcal{D}},\tilde{\mathcal{F}},\tilde{\mathcal{G}}$ representing $\mathcal{H}_{\boldsymbol{\epsilon}}$ [Eq. (5c)] take the forms

$$\mathcal{A} = a(\epsilon_1), \tag{9a}$$

$$\mathcal{B}(\tilde{\mathcal{B}}) = b(\tilde{b})(\epsilon_2 \quad s\text{-}\epsilon_3), \tag{9b}$$

$$\mathcal{C} = c(\epsilon_4 \quad \epsilon_5 \quad \epsilon_6), \tag{9c}$$

$$\mathcal{D} = d\begin{pmatrix} 2\epsilon_{xx} - \epsilon_{yy} - \epsilon_{zz} & 0 & 0 \\ 0 & -\epsilon_{xx} + 2\epsilon_{yy} - \epsilon_{zz} & 0 \\ 0 & 0 & -\epsilon_{xx} - \epsilon_{yy} + 2\epsilon_{zz} \end{pmatrix}, \tag{9d}$$

$$\tilde{\mathcal{D}} = \tilde{d}\begin{pmatrix} \epsilon_{yy} - \epsilon_{zz} & 0 & 0 \\ 0 & -\epsilon_{xx} + \epsilon_{zz} & 0 \\ 0 & 0 & \epsilon_{xx} - \epsilon_{yy} \end{pmatrix},$$

$$\mathcal{E} = e\begin{pmatrix} 0 & \epsilon_3 \\ \epsilon_2 & 0 \end{pmatrix}, \tag{9e}$$

$$\mathcal{F}(\tilde{\mathcal{F}}) = f(\tilde{f})\begin{pmatrix} \omega\epsilon_6 & \omega^*\epsilon_5 & \epsilon_4 \\ s\text{-}\omega^*\epsilon_6 & s\text{-}\omega\epsilon_5 & s\text{-}\epsilon_4 \end{pmatrix}, \tag{9f}$$

$$\mathcal{G} = g\begin{pmatrix} 0 & \epsilon_6 & \epsilon_5 \\ \epsilon_6 & 0 & \epsilon_4 \\ \epsilon_5 & \epsilon_4 & 0 \end{pmatrix},$$

$$\tilde{\mathcal{G}} = \tilde{g}\begin{pmatrix} 0 & -i\epsilon_6 & i\epsilon_5 \\ i\epsilon_6 & 0 & -i\epsilon_4 \\ -i\epsilon_5 & i\epsilon_4 & 0 \end{pmatrix}, \tag{9g}$$

where $\mathcal{A}$ has the dimension of the involved irreducible representation ($\omega^3=1$, $s\text{-}=-1$ for tilde blocks, 1 otherwise). Historically, matrix blocks $\mathcal{D}$ and $\mathcal{G}$, which correspond to valence-bandlike couplings, were first derived by Bir and Pikus.[10] The conduction-valence bands-like coupling $\mathcal{C}$ was introduced in the eight-band model of Ref. 18.

Both operators $\mathcal{H}_{\mathbf{k}\mathrm{so}}$ and $\mathcal{H}'_{\boldsymbol{\epsilon}\mathrm{so}}$ [Eqs. (5d) and (5e)] act on the new basis tensor product of the previous basis and the $\{\uparrow\downarrow\}$ electron-spin basis. The matrix forms of the coupling blocks $\mathcal{X},\mathcal{Y},\tilde{\mathcal{Y}},\mathcal{Z},\tilde{\mathcal{Z}}$ and $\mathcal{U},\mathcal{S},\tilde{\mathcal{S}},\mathcal{T},\tilde{\mathcal{T}}$ are thus again derived from simple group analysis in the tensorial basis.

The operator ∇V_0 transforms such as T_2 in the T_d symmetry group (T_{1u} in O_h). Consequently, the blocks $\mathcal{X},\mathcal{Y},\mathcal{Z}$ and $\tilde{\mathcal{Y}},\tilde{\mathcal{Z}}$ of $\mathcal{H}_{\mathbf{k}\mathrm{so}}$ are, respectively, similar to the blocks $\mathcal{P},\mathcal{Q},\mathcal{R}$ and $\tilde{\mathcal{Q}},\tilde{\mathcal{R}}$ of $\mathcal{H}_{\mathbf{K}_{\boldsymbol{\epsilon}}\cdot\mathrm{p}}$, see expressions in Eqs. (7), with the scalar vector $\mathbf{K}_{\boldsymbol{\epsilon}}=(1-\boldsymbol{\epsilon})\mathrm{k}$ formally replaced by the vectorial spin-dependent operator $\mathbf{K}=[\mathrm{k},\boldsymbol{\sigma}]$ in the tensorial basis. The coefficients of blocks $\mathcal{X}$, $\mathcal{Y}$, and $\mathcal{Z}$ are labeled χ, ϕ, and ξ, respectively. However, in contrast with $Q(\tilde{Q})$, the coefficient $\phi(\tilde{\phi})$ does not vanish inside a same degenerate level. In particular, it leads to linear-k terms in the valence band of zincblende structures. Compared to Ref. 9, one has the correspondence $\phi=-2\sqrt{3}\mathrm{C}$.

The first term in $\mathcal{H}_{\boldsymbol{\epsilon}\mathrm{so}}$ is negligible compared to the two others.[18] Ignoring this term, the operator $\mathcal{H}'_{\boldsymbol{\epsilon}\mathrm{so}}$ can be written in a form analogous to that of $\mathcal{H}_{\mathrm{so}}$

$$\mathcal{H}'_{\boldsymbol{\epsilon}\mathrm{so}} = \frac{\hbar}{4m_0c^2}[\nabla V_0, \mathrm{p}] \cdot \boldsymbol{\Sigma}_{\boldsymbol{\epsilon}} \tag{10}$$

with

$$\begin{cases} \Sigma_{\epsilon_x} = (1 - \epsilon_{yy} - \epsilon_{zz})\sigma_x + \epsilon_{xy}\sigma_y + \epsilon_{xz}\sigma_z \\ \Sigma_{\epsilon_y} = \epsilon_{xy}\sigma_x + (1 - \epsilon_{xx} - \epsilon_{zz})\sigma_y + \epsilon_{yz}\sigma_z \\ \Sigma_{\epsilon_z} = \epsilon_{zx}\sigma_x + \epsilon_{yz}\sigma_y + (1 - \epsilon_{xx} - \epsilon_{yy})\sigma_z \end{cases}. \tag{11}$$

The operator $[\nabla V_0,\mathrm{p}]$ transforms like an axial vector according to the T_1 representation in the T_d symmetry group (T_{1g} in O_h).

$$\mathcal{U} = \frac{\Upsilon}{\sqrt{3}}(\Sigma_{\epsilon_x} \quad \Sigma_{\epsilon_y} \quad \Sigma_{\epsilon_z}), \tag{12a}$$

$$\mathcal{S} = \frac{\Delta}{3}\begin{pmatrix} 0 & -i\Sigma_{\epsilon_z} & i\Sigma_{\epsilon_y} \\ i\Sigma_{\epsilon_z} & 0 & -i\Sigma_{\epsilon_x} \\ -i\Sigma_{\epsilon_y} & i\Sigma_{\epsilon_x} & 0 \end{pmatrix}, \tag{12b}$$

$$\tilde{\mathcal{S}} = \frac{\tilde{\Delta}}{3}\begin{pmatrix} 0 & \Sigma_{\epsilon_z} & \Sigma_{\epsilon_y} \\ \Sigma_{\epsilon_z} & 0 & \Sigma_{\epsilon_x} \\ \Sigma_{\epsilon_y} & \Sigma_{\epsilon_x} & 0 \end{pmatrix},$$

$$\mathcal{T}(\tilde{\mathcal{T}}) = \frac{\Theta(\tilde{\Theta})}{\sqrt{3}}\begin{pmatrix} \omega\Sigma_{\epsilon_x} & \omega^*\Sigma_{\epsilon_y} & \Sigma_{\epsilon_z} \\ s\text{-}\omega^*\Sigma_{\epsilon_x} & s\text{-}\omega\Sigma_{\epsilon_y} & s\text{-}\Sigma_{\epsilon_z} \end{pmatrix} \tag{12c}$$

($s\text{-}=-1$ for tilde blocks, 1 otherwise). Like for the $\mathcal{H}_{\mathbf{K}_{\boldsymbol{\epsilon}}\cdot\mathrm{p}}$ term, all parameters contribute to both strained and unstrained structure descriptions. Coefficients Υ, Δ, and Θ have been defined to give simple diagonal contributions in the latter case (in the double group, the spin-orbit coupling transforms such as A_1), using the simple group basis combinations

$$E_{5/2(1/2)}\left\{\frac{i}{\sqrt{3}}((X+iY)\downarrow + Z\uparrow), \frac{i}{\sqrt{3}}((X-iY)\uparrow - Z\downarrow)\right\} \leftarrow T_{2(1)},$$

$$E_{1/2(5/2)}\{a_{1(2)}\uparrow, a_{1(2)}\downarrow\} \leftarrow A_{1(2)},$$

$$F_{3/2}\left\{\frac{i}{\sqrt{2}}(e_1+e_2)\downarrow,\frac{1}{\sqrt{2}}(e_1-e_2)\uparrow,-\frac{1}{\sqrt{2}}(e_1-e_2)\downarrow,-\frac{i}{\sqrt{2}}(e_1+e_2)\uparrow\right\}\leftarrow E,$$

$$F_{3/2}\left\{-\frac{i}{\sqrt{2}}(X+iY)\uparrow,\frac{i}{\sqrt{3}}\left(\sqrt{2}Z\uparrow-\frac{1}{\sqrt{2}}(X+iY)\downarrow\right),\frac{i}{\sqrt{3}}\left(\sqrt{2}Z\downarrow+\frac{1}{\sqrt{2}}(X-iY)\uparrow\right),\frac{i}{\sqrt{2}}(X-iY)\downarrow\right\}\leftarrow T_{2(1)},\tag{13}$$

where X,Y,Z refer to the basis functions of either T_1 or T_2. Indeed, Δ represents the energy shift between $F_{3/2}$ and $E_{5/2}$ originating from the splitting of T_2 when spin is added, usually referred to the spin-orbit energy of the valence band. Moreover, the impacts of the spin splitting Δ^- between the p-like valence band and second conduction band have been pointed out[19] while its value is still discussed.[20] Similarly, Υ and Θ are the block-diagonal-energy corrections due to the spin-orbit coupling in $E_{5/2}$ or $E_{1/2}$, and $F_{3/2}$, respectively.

A k·p model is constructed by projecting the operator $\mathcal{H}$ on a finite dimension basis. Due to the basis restriction that unique step actually corresponds to a first-order treatment. Nevertheless, once the basis is chosen, it is possible to include the effects of the remote bands, distinguished by the subscript ν, by performing a second-order renormalization.[21,22] The procedure reads with the formal writing

$$\mathcal{H}_{ij}\leftarrow\mathcal{H}_{ij}+\sum_{\nu\neq i,j}\frac{1}{2}\left\{\frac{1}{E_i-E_\nu}+\frac{1}{E_j-E_\nu}\right\}\mathcal{H}_{i\nu}\mathcal{H}_{\nu j},\tag{14}$$

where only i,j belong to the basis restriction. Using the previous results, it is straightforward, but demanding especially in the strained case, to determine the matrix forms of the second-order corrections throughout the $\mathcal{H}_{i\nu}$ and $\mathcal{H}_{\nu j}$ coupling terms.

III. APPLICATIONS

A. Full-zone k·p models

Semiconductor structures are the basis components of a nano(opto)electronics in which the device working is mainly controlled by the structural microscopic organization. In highly perturbed semiconductor structures, carriers are likely to explore large regions of the Brillouin zone. Simplest k·p models fail in simulating this behavior. Therefore, understanding of future device architectures is subjected to the development of k·p models with a high number of bands to allow accurate descriptions of the full Brillouin zone.

In 1960s, Cardona and Pollak[1] published the first 30-band k·p model for unstrained diamond structure semiconductors, $\mathcal{H}\equiv\mathcal{H}_0+\mathcal{H}_{\text{k·p}}$. All spin-orbit terms were ignored, hence the Bloch basis at the Γ point reduced to only 15 spinless functions $\{A_1,T_2,E,A_1,T_2,A_1,T_2,A_1\}$ (see Table IV). Only coupling blocks of types $\mathcal{P}$, $\mathcal{Q}$, and $\mathcal{R}$ form the model. For the first time, any second-order renormalization was necessary to give satisfying band-structure results in the main directions of the whole Brillouin zone. Such a full-zone approach that ignores the remote bands was corroborated by pseudopotential calculations.[23] This early work inspired very recent developments. In 2004, the model was extended by Richard *et al.*[2,24] to zincblende structure semiconductors including the spin-dependent k-independent H_{so} term. New blocks of type $\mathcal{S}$ were added to the previous model and the coupling term $\mathcal{T}$ was presented. The energy bands of Si, Ge, and GaAs crystals were obtained throughout the entire Brillouin zone. However, for energies about 6 eV above the gap, one band coming from the $\langle 220\rangle$ fold point is still missing. This lack would justify attempt to the 54-band model. The same year, the full-zone treatment was developed for crystals of wurtzite structure which corresponds to the C_{6v} point group.[3] Strain issue was first addressed by Bir and Pikus.[10] The matrix sum $\mathcal{A}+\mathcal{D}+\mathcal{G}$ representing $\mathcal{H}_{\boldsymbol{\epsilon}}$ within the valence-band forms the so-called Bir-Pikus Hamiltonian (the original coefficients l,n,m are linear combinations of the a,d,g ones). That six-band model is still widely used to account for strain effects in cubic crystals.[25] In the nineties, the eight-band k·p model was derived for strained zincblende crystals.[18] The new interaction matrix $\mathcal{C}$ involving the conduction band was calculated using second-order Löwdin perturbation theory.[22] Strain contributions in $\mathcal{H}'_{\boldsymbol{\epsilon}\text{so}}$ originating from the spin-orbit interaction in the Hamiltonian were also considered for the first time. The author showed that unique coefficients Υ and Δ are need to represent both $\mathcal{H}_{\boldsymbol{\epsilon}\text{so}}$ and $\mathcal{H}_{\text{so}}$. Very recently, generalized Bir-Pikus approaches were proposed for the 20- and the 30-band models. First, only interaction matrices between bands of the same symmetry of the valence band (valence-bandlike couplings) were reproduced in the whole 30×30 matrix.[2,24] Very recently, new coupling blocks of type $\mathcal{B}$, $\mathcal{E}$, and $\mathcal{F}$ coming from the orbital part $\mathcal{H}_{\boldsymbol{\epsilon}}$ of the strain Hamiltonian were derived for diamond-structure semiconductors.[4,26] Full-zone k·p models are still missing the coupling blocks representing the linear-k term $\mathcal{H}_{\text{kso}}$ and the strain contribution $\mathcal{H}'_{\boldsymbol{\epsilon}\text{so}}$ introduced by the spin-orbit interaction. Moreover, descriptions of strained zincblende structures never go beyond the six-band model of Bir-Pikus for $\mathcal{H}_{\boldsymbol{\epsilon}}$: only coupling blocks of type $\mathcal{A}$, $\mathcal{D}$, and $\mathcal{G}$ enter the full-zone model.

Using results of Sec. II, it is straightforward to complete the 30×30 matrix representation of $\mathcal{H}$ in the $\{A_1>T_2>E>A_1>T_2>A_1>T_2>A_1\}\otimes\{\uparrow,\downarrow\}$ basis for zincblende crystals.[1] Operators $\mathcal{H}_{\text{kso}}$ and $\mathcal{H}_{\text{k·p}}$ transform according to the same irreducible representation, hence are

TABLE IV. Irreducible representations associated to the spinless Bloch functions at the Γ point. The perturbation basis $\langle hkl\rangle$ (degeneracy) of the orthogonal plane waves $\langle e^{i(hk_x+kk_y+lk_z)}\rangle$ are recalled in the first row.

OPW	$\langle 000\rangle$ (1)	$\langle 111\rangle$ (8)	$\langle 200\rangle$ (6)	$\langle 220\rangle$ (12)
T_d	A_1	A_1,T_2	A_1,E,T_2	A_1,T_1,E
O_h	A_{1g}	$A_{1g},A_{2u},T_{2g},T_{1u}$	A_{2u},E_u,T_{2g}	A_1,T_{2g},T_{1u},E_g

TABLE V. New coupling terms in the fifty-four model for diamond structure semiconductors.

	A_{1g}	A_{2u}	E_g	E_u	T_{1u}	T_{2g}
E_g	$\mathcal{B}$		$\mathcal{E}$		$\mathcal{R},\mathcal{Z}$	$\tilde{\mathcal{T}},\mathcal{F}$

represented by similar matrices. For $\mathcal{H}_{\boldsymbol{\epsilon}}$, the matrix takes the form

$$\begin{bmatrix} \mathcal{A} & \mathcal{C}' & \mathcal{B} & \mathcal{A}' & \mathcal{C} & \mathcal{A} & \mathcal{C}' & \mathcal{A}' \\ & \mathcal{H}_{\mathcal{BP}} & \mathcal{F}'^{\dagger} & \mathcal{C}^{\dagger} & \mathcal{H}'_{\mathcal{BP}} & \mathcal{C}'^{\dagger} & \mathcal{H}_{\mathcal{BP}} & \mathcal{C}^{\dagger} \\ & & \mathcal{H}_{\mathcal{D}} & \mathcal{B}'^{\dagger} & \mathcal{F} & \mathcal{B}^{\dagger} & \mathcal{F}' & \mathcal{B}'^{\dagger} \\ & & & \mathcal{A} & \mathcal{C}' & \mathcal{A}' & \mathcal{C} & \mathcal{A} \\ & & & & \mathcal{H}_{\mathcal{BP}} & \mathcal{C} & \mathcal{H}'_{\mathcal{BP}} & \mathcal{C}' \\ & & \text{H.c.} & & & \mathcal{A} & \mathcal{C}' & \mathcal{A}' \\ & & & & & & \mathcal{H}_{\mathcal{BP}} & \mathcal{C}^{\dagger} \\ & & & & & & & \mathcal{A} \end{bmatrix}, \quad (15)$$

where $\mathcal{H}_{\mathcal{D}}=\mathcal{A}+\mathcal{C}$ is the strain Hamiltonian inside the E (d-like) band and $\mathcal{H}_{\mathcal{BP}}=\mathcal{A}+\mathcal{B}+\mathcal{G}$ is the Bir-Pikus Hamiltonian (matrix forms). For $\mathcal{H}'_{\boldsymbol{\epsilon}\text{so}}$

$$\begin{bmatrix} 0 & 0 & 0 & 0 & 0 & 0 & 0 & 0 \\ & \mathcal{S} & \tilde{\mathcal{T}}^{\dagger\prime} & 0 & \mathcal{S}' & 0 & \mathcal{S} & 0 \\ & & 0 & 0 & \tilde{\mathcal{T}} & 0 & \tilde{\mathcal{T}}' & 0 \\ & & & 0 & 0 & 0 & 0 & 0 \\ & & & & \mathcal{S} & 0 & \mathcal{S}' & 0 \\ & & \text{H.c.} & & & 0 & 0 & 0 \\ & & & & & & \mathcal{S} & 0 \\ & & & & & & & 0 \end{bmatrix}, \quad (16)$$

where H.c. stands for Hermitian conjugation. Two identical blocks are nevertheless distinguishing by two different $\mathbf{k}\cdot\mathbf{p}$ parameters. In the $\{A_{2u},T_{2g},E_u,A_{1g},T_{1u},A_{2u},T_{2g},A_{1g}\}\otimes\{\uparrow,\downarrow\}$ basis, all quoted parameters, e.g., b' and Δ', related to the quoted blocks, e.g., $\mathcal{B}'$ and $\mathcal{S}'$, are zero due to *ugg* parity rules. Moreover, the change $(e_1,e_2)\rightarrow(e_1,-e_2)$ has been made in the E_u subspace (see Table I). Such basis changes are often used to provide similar matrix forms in O_h and T_d symmetry groups. Here, it allows $(\tilde{\mathcal{B}},\tilde{\mathcal{F}},\mathcal{T})\rightarrow(\mathcal{B},\mathcal{F},\tilde{\mathcal{T}})$ in O_h. Furthermore, different basis were used in previous works.[2,4] For the sake of completeness, we give here the related transformations: $D_1=i(e_1+e_2)/\sqrt{2}$ and $D_2=(e_2-e_1)/\sqrt{2}$ for Ref. 2 and $D_1=\frac{\sqrt{3}}{\omega-1}e_1+\frac{\sqrt{3}}{1-\omega^*}e_2$ and $D_2=i(\frac{1-\omega^*}{\sqrt{3}}e_1+\frac{1-\omega}{\sqrt{3}}e_2)$ for Ref. 4.

It is as easy to obtain the 54×54 matrix representation of $\mathcal{H}$ in the extended basis.[27] From the point of view of group theory, the only difference lies in the O_h symmetry group. Indeed, the irreducible representation E_g appears in the new basis. All new coupling terms, compared to the 30-band model, are summarized in Table V.

It is worth to underscore that the set of fitted parameter values for a given multiband $\mathbf{k}\cdot\mathbf{p}$ model implicitly accounts for all the ignored contributions, such as higher energy-band effects or neglected interactions. So that, any improvement of the empirical description would require new fitting procedures.

B. Zincblende ZnO oxide

ZnO-based systems are regarded as good candidates for future electronics, see reviews of Refs. 13 and 28. However, challenges still stand even about deep understanding of the electronic properties in bulk ZnO.[29,30] One of the most striking peculiarities is the fine structure of the valence-band maximum, whose reversed ordering is still a subject of controversy, both in the zincblende and the wurtzite-type ZnO crystals.[31] The anomalous sequence at the valence-band maximum, $E_{5/2}>F_{3/2}$ in T_d and $E_{1/2}>E_{3/2}>E_{1/2}$ in C_{6v} (see Table VI),[32] has been attributed to an effective negative spin-orbit splitting. The reason for that splitting inversion consists in the hybridization of the oxygen $2p$ states with the Zn $3d$ states[11,12] which are completely filled and lie experimentally at about 7 eV below the upper valence-band edge.[31] Nevertheless the d-like bands may influence the fine structure of the p-like valence-band maximum throughout a dramatic pd-like spin-orbit coupling.

We propose a new $\mathbf{k}\cdot\mathbf{p}$ model able to account for the unusual spin-orbit effects at the ZnO valence-band maximum. The basis is extended to 16 states to include the lower-

TABLE VI. Calculated fine structure of the valence-band edge at the Γ point of ZnO. The energy zero is at the minimum of the conduction band. The spin degeneracy is included for the scalar relativistic case.

Crystal structure	Method	Energies (eV)	Degeneracy	Symmetry [Ref. 14 (Ref. 15)]
Zincblende	Scalar relativistic	−0.7830	6	T_2 (Γ_5)
Zincblende	Full relativistic	−0.7568	2	$E_{5/2}$ (Γ_7)
		−0.7937	4	$F_{3/2}$ (Γ_8)
Wurtzite	Scalar relativistic	−0.9349	4	E (Γ_5)
		−1.0094	2	A_1 (Γ_1)
Wurtzite	Full relativistic	−0.9156	2	$E_{1/2}$ (Γ_7)
		−0.9484	2	$E_{3/2}$ (Γ_9)
		−1.0102	2	$E_{1/2}$ (Γ_7)

lying *d*-like bands. Band structure results show that there are no other bands in the corresponding energy region which extends up to about 6 eV below the Fermi level.[31] The *d*-like valence bands are currently avoided from the basis of most k·p models used for ZnO-based compounds. In wurtzite-type ZnO, the six states of the valence-band maximum are described by the six-band Rashba-Sheba-Pikus model derived in the C_{6v} point group or the simplified quasicubic Kohn-Luttinger model in which the wurtzite structure is regarded as a deformed (quasi)cubic one (see Ref. 10 for both effective Hamiltonians). In zincblende-type ZnO, the usual Kohn-Luttinger model is used.[21] However in such descriptions, only energies at the valence-band maximum can be reproduced throughout the empirical k·p parameter values, e.g., $\Delta<0$ in the Kohn-Luttinger model to account for the negative sign of the effective spin-orbit splitting. It follows that band mixing as well as interplay between the different terms of the Hamiltonian are completely ignored.

The 16-band spin-orbit model is developed for ZnO in zincblende structure. States originating from the Zn 3*d* levels correspond to the E and $T_2^{(1)}$ irreducible representations of the T_d symmetry group, leading to $E_{5/2}^{(1)}$, $F_{3/2}$, and $F_{3/2}^{(1)}$ in the double group. These functions are added to the standard basis of the Kohn-Luttinger model, here referred as $F_{3/2}^{(2)}$ and $E_{5/2}^{(2)}$. The spin-orbit matrix at the Γ point is merely obtained from previous developments. In the basis of Eq. (13), it reads

$$\begin{pmatrix} F_{3/2}^{(2)} & E_{5/2}^{(2)} & E_{5/2}^{(1)} & F_{3/2} & F_{3/2}^{(1)} \\ E_2+\zeta_2 & 0 & 0 & \Theta_2 & \zeta_{12} \\ & E_2-2\zeta_2 & -2\zeta_{12} & 0 & 0 \\ & & E_1+2\zeta_1 & 0 & 0 \\ & \text{c.c.} & & E_1' & \Theta_1 \\ & & & & E_1-\zeta_1 \end{pmatrix} \quad (17)$$

using $\zeta_{1,2,12}=\Delta_{1,2,12}/3$ for convenience with $\zeta_{1,2,12}>0$. Scalar coefficients are implicitly multiplied by identity matrices of dimension 2 for $E_{5/2}$ and 4 for $F_{3/2}$ representations (c.c. stands for complex conjugation). The $E_{5/2}$ and $F_{3/2}$ bands are uncoupled at $\mathbf{k}=\mathbf{0}$ but have common parameters arising from spinless part. Such a form already accounts for a reversed level order in the two T_2 bands: the level of $E_{5/2}^{(1)}$ is higher than that of $F_{3/2}^{(1)}$ in the *d* orbital.[33]

The 16-band model exhibits three *pd*-like spin-orbit couplings, namely, $\Theta_{1,2}$ coming from T_2-E interband terms and ζ_{12} coming from T_2-T_2 interband term. Only ζ_{12} induces a repulsion between the two $E_{5/2}$ bands and hence supports the occurrence of a splitting inversion, in agreement with earlier tight-binding developments[33] and first principles calculations.[11] Indeed, the spin-orbit interaction couples states of same symmetry but the coupling strength is four times bigger for $E_{5/2}$ than for $F_{3/2}$. As a result, the lower-lying *d*-like bands give a negative contribution to the effective spin-orbit splitting. That qualitative analysis is illustrated in Fig. 1. The valence-band energies at the Γ point are represented as a function of the spin-orbit parameter ζ_{12}. The usual ordering occurs at $\zeta_{12}=0$. For $\zeta_{12}^2<\Delta E\times\zeta_2$, the energy separation between $F_{3/2}^{(2)}$ and $E_{5/2}^{(2)}$ bands is reduced; for $\zeta_{12}^2>\Delta E\times\zeta_2$, $F_{3/2}^{(2)}$, and $E_{5/2}^{(2)}$ bands cross, giving rise to a

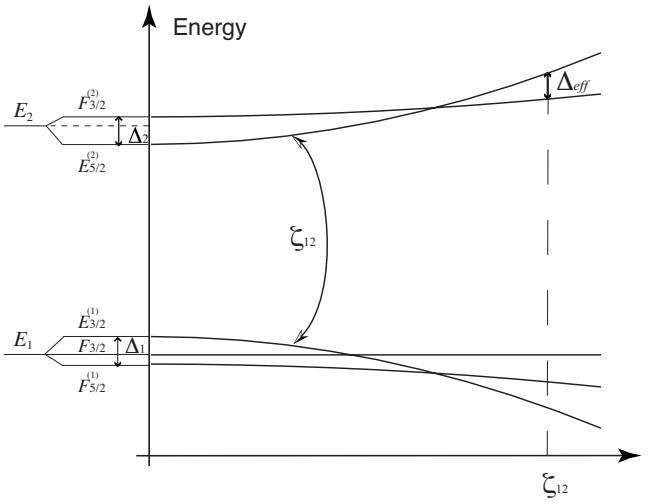

FIG. 1. Schematic energy diagram at k=0 as a function of the spin-orbit coupling parameter ζ_{12} (here $\Theta_{1,2}\approx 0$, $\zeta_1\approx\zeta_2$, and $E_1'\approx E_1$).

negative effective spin-orbit splitting Δ_{eff}. Besides, the proposed model also supplies the band-gap reduction expected from first principles calculations[11] since the valence-band maximum energies increase as a function of ζ_{12}. Moreover, a strong interband coupling ζ_{12} implies a strong interband mixing between the *d*-like and the *p*-like valence bands, which we propose to evaluate.

For a quantitative analysis, we first calculate the fine structure of the valence-band edge using the local-density approximation (LDA) in its fully relativistic version. More in detail, we use the full-potential local-orbital (FPLO, version FPLO7) band-structure scheme,[34] taking into account spin-orbit coupling by its relativistic version (RFPLO).[35] In the FPLO method a minimum basis approach is employed, which allows for accurate and efficient calculations. There are no shape restrictions to the crystal potential, the site-centered potentials and densities were expanded in spherical harmonics up to $l_{\max}=12$. The LDA parametrization of Perdew and Wang was used.[36] In the RFPLO method, the four-component Kohn-Sham-Dirac equation for the crystal, which includes spin-orbit coupling to all orders, is solved in a collinear approximation. The scheme was recently applied to calculate the magnetocrystalline anisotropy energy of transition-metal compounds[37] in good agreement with experiment and state-of-the-art calculations. For ZnO, a *k* mesh of (12,12,12) was used in all calculations which guaranties sufficient accuracy. We used the experimental lattice parameters in both structures which are $a=4.557$ Å for zincblende, and $a=3.2427$ Å and $c=5.1948$ Å with the internal parameter $u=0.3826$ for the wurtzite structure.

We confirm the reversed order at the valence-band maximum for both crystalline structures, which coincides with previous studies.[31] Results are summarized in Table VI. The energies at the valence-band edge without and with spin-orbit coupling are compared for both crystalline structures. The LDA energy gap underestimates the experimental value of about 3.3 eV considerably which is a known drawback of LDA. Another drawback is the position of the Zn 3*d* levels

which lie in the LDA calculation at about 5–6 eV below the valence-band maximum, slightly too high with respect to experiment.[38] The amount of the level inversion in the zincblende structure of about 40 meV corresponds to literature values.[29,31] The LDA level splitting for both zincblende and wurtzite structures overestimates the experimental data. The reason is the underestimated distance between valence band and Zn $3d$ states. We obtain $\Delta E^{ab\ initio}=5.897$ eV and $\Delta_{eff}^{ab\ initio}=0.037$ eV.

To demonstrate the usefulness of the extended valence-band model, we put the focus on ζ_{12}: couplings between $F_{3/2}^{(1,2)}$ and $F_{3/2}$ are ignored,[33] $\Theta_{1,2}=0$, we assume $E_1'=E_1$, and we use the perturbation condition $\Delta E=E_2-E_1 \gg \zeta_{1,2}=0$.[33] Fitting the simplified $\mathbf{k}\cdot\mathbf{p}$ model, we estimate $\zeta_{12}\approx 250$ meV. Such a spin-orbit parameter leads to a *pd*-like hybridization of about 10% which corresponds to literature values (between 10% and 30%).[38–41] That *pd*-like hybridization should have dramatic consequences even with magnetic impurities and hence should be described by the 16-band model in empirical approach. In particular, the reliability of the six-band model has to be surveyed even in the C_{6v} group.

The model we developed can be compared to the ten-band $\mathbf{k}\cdot\mathbf{p}$ model achieved for diluted nitride alloys of III-V semiconductors.[8] The strong negative band-gap bowing effects in Ga(N)As were fairly reproduced by including a *s*-like higher-lying band formed by nitrogen resonant states in the usual eight-band $\mathbf{k}\cdot\mathbf{p}$ basis. The ten-band approach is presently used to exhibit the markedly different electronic properties in low dimensional systems of diluted nitride III-V alloys with respect to conventional III-V alloys. As a recent example, the influence of the nitrogen composition on the electronic properties under electric field was investigated in In(N)Sb nanowires using the ten-band model.[42] In comparison, the model we developed could be seen as a basis for next $\mathbf{k}\cdot\mathbf{p}$ models including the effects of the wurtzite structure for ZnO, conduction-valence-band mixings, and *spd-d* exchange interactions for Zn(Mn,Co)O diluted magnetic oxides which are raising more and more debates in the field of semiconductor spintronics,[43] in particular, on their promising high T_C ferromagnetism recently predicted.[44]

IV. CONCLUSION

A synthesis work on $\mathbf{k}\cdot\mathbf{p}$ models in strained zincblende crystal was presented to supply the theoretical material required for next developments in the $\mathbf{k}\cdot\mathbf{p}$ theory framework. In particular, strain-induced contributions were included in the latest full-zone 30-band approaches which provide descriptions of the whole Brillouin zone. The 54-band model was also considered in the workable approach we proposed. Besides, a 16-band model was constructed for the ZnO valence-band maximum by adding the lower-lying *d*-like bands in standard description. We demonstrated that empirical model to be able to reproduce the intimate structure of the valence-band maximum: inversion of the spin-orbit splitting and *pd*-like interband mixing. The key spin-orbit parameter and the resulting state hybridization were determined by the means of relativistic LDA calculations. Finally, external effects driven by electric or magnetic fields should be considered in future methodological developments.

ACKNOWLEDGMENTS

This work was supported by the ANR project MODERN (Grant No. ANR-05-NANO-002), the DNIPRO project 1482XB and the PICS project 4767. Also, one of the authors (R.H.) thanks S. Ryabchenko for useful discussions.

*fabienne.michelini@univ-provence.fr

[1] M. Cardona and F. H. Pollak, Phys. Rev. **142**, 530 (1966).
[2] S. Richard, F. Aniel, and G. Fishman, Phys. Rev. B **70**, 235204 (2004).
[3] R. Beresford, J. Appl. Phys. **95**, 6216 (2004).
[4] D. Rideau, M. Feraille, L. Ciampolini, M. Minondo, C. Tavernier, H. Jaouen, and A. Ghetti, Phys. Rev. B **74**, 195208 (2006).
[5] E. O. Kane, J. Phys. Chem. Solids **1**, 249 (1957).
[6] C. R. Pidgeon and R. N. Brown, Phys. Rev. **146**, 575 (1966).
[7] U. Rössler, Solid State Commun. **49**, 943 (1984).
[8] E. P. O'Reilly and A. Lindsay, Phys. Status Solidi B **216**, 131 (1999).
[9] G. Dresselhaus, Phys. Rev. **100**, 580 (1955).
[10] G. L. Bir and G. E. Pikus, *Symmetry and Strain-Induced Effects in Semiconductors* (Wiley, New York, 1974).
[11] S.-H. Wei and A. Zunger, Phys. Rev. B **37**, 8958 (1988).
[12] S.-H. Wei and A. Zunger, Phys. Rev. B **49**, 14337 (1994).
[13] U. Özgür, Y. I. Alinov, C. Liu, A. Teke, M. A. Reshchikov, S. Dogan, V. Avrutin, S.-J. Cho, and H. Morkoc, J. Appl. Phys. **98**, 041301 (2005).
[14] S. L. Altmann and P. Herzig, *Point-Group Theory Tables* (Clarendon, Oxford, 1994).
[15] G. F. Koster, J. O. Dimmock, R. G. Wheeler, and H. Statz, *Properties of the Thirty-Two Point Groups* (MIT, Cambridge, MA, 1963).
[16] For a given coupling term Ξ of $\mathcal{H}$ that transforms accordingly as the irreducible representation Γ_k, one block represents the coupling matrix in between states that transform accordingly as Γ_j and $\Gamma_{j'}$ at the Γ point. Following the generalized Wigner-Eckart theorem (Ref. 45), the coupling is written as a linear combination of the $\{\langle jm|j'm'kq\rangle\}_{mm'}$ Clebsch-Gordan matrices, where $|kq\rangle$, $|jm\rangle$, and $|j'm'\rangle$ are the standard bases that transform, respectively, such as Γ_k, Γ_j, and $\Gamma_{j'}$ under any operation of the considered symmetry group (see Ref. 14 for details). Coefficients correspond to reduced matrix elements that are independent of m, q, and m'. The number of combination coefficients is directly given by the T_d multiplication table. In the O_h group, an additional selection rule plays: any coefficient becomes zero as soon as products of type *uuu* or *ugg* occur in the expectation value of the Hamiltonian term.

[17] Strictly, involved parameters, e.g., P, differ from the reduced matrix elements (Ref. 45). Prefactors are included.
[18] T. B. Bahder, Phys. Rev. B **41**, 11992 (1990).
[19] M. Cardona, N. E. Christensen, and G. Fasol, Phys. Rev. B **38**, 1806 (1988).
[20] J.-M. Jancu, R. Scholz, E. A. de Andrada e Silva, and G. C. La Rocca, Phys. Rev. B **72**, 193201 (2005).
[21] J. M. Luttinger and W. Kohn, Phys. Rev. **97**, 869 (1955).
[22] P.-O. Löwdin, J. Math. Phys. **3**, 969 (1962).
[23] L.-W. Wang and A. Zunger, Phys. Rev. B **54**, 11417 (1996).
[24] S. Richard, F. Aniel, and G. Fishman, Phys. Rev. B **71**, 169901(E) (2005).
[25] J. Bhattacharyya and S. Ghosh, Phys. Status Solidi A **204**, 439 (2007).
[26] In Ref. 4, the four coefficients $a_{12}, b_{12}, c_{12}, d_{12}$ are not linearly independent. Only two parameters, respectively, a and e, are needed to account for the strain coupling $\mathcal{H}_{\boldsymbol{\epsilon}}$ in between E states.
[27] F. Bassani and M. Yoshimine, Phys. Rev. **130**, 20 (1963).
[28] C. Klingshirn, Phys. Status Solidi B **244**, 3027 (2007).
[29] S. Z. Karazhanov, P. Ravindran, A. Kjekshus, H. Fjellvag, and B. G. Svensson, Phys. Rev. B **75**, 155104 (2007).
[30] J. Fu, P. Liu, J. P. Cheng, A. S. Bhalla, and R. Guo, Appl. Phys. Lett. **90**, 212907 (2007).
[31] W. R. L. Lambrecht, A. V. Rodina, S. Limpijumnong, B. Segall, and B. K. Meyer, Phys. Rev. B **65**, 075207 (2002).
[32] The ZnO compound belongs to the II-VI semiconductor type and crystallizes in both zincblende and wurtzite structures. In the latter, the three space directions are no longer equivalent: the T_2 representation of T_d splits into two representations, A_1 and E_1 of the C_{6v} point group, $E_{1/2}$ and $E_{1/2} \oplus E_{3/2}$ in the double group (Ref. 14) with corresponding crystal-field and spin-orbit splittings.
[33] K. Shindo, A. Morita, and H. Kamimura, J. Phys. Soc. Jpn. **20**, 2054 (1965).
[34] K. Koepernik and H. Eschrig, Phys. Rev. B **59**, 1743 (1999).
[35] I. Opahle, S. Elgazzar, K. Koepernik, and P. M. Oppeneer, Phys. Rev. B **70**, 104504 (2004).
[36] J. P. Perdew and Y. Wang, Phys. Rev. B **45**, 13244 (1992).
[37] D. Mertz, R. Hayn, I. Opahle, and H. Rosner, Phys. Rev. B **72**, 085133 (2005).
[38] A. R. H. Preston, B. J. Ruck, L. F. J. Piper, A. DeMasi, K. E. Smith, A. Schleife, F. Fuchs, F. Bechstedt, J. Chai, and S. M. Durbin, Phys. Rev. B **78**, 155114 (2008).
[39] M. Usuda, N. Hamada, T. Kotani, and M. van Schilfgaarde, Phys. Rev. B **66**, 125101 (2002).
[40] A. Janotti, D. Segev, and C. G. Van de Walle, Phys. Rev. B **74**, 045202 (2006).
[41] P. Schröer, P. Krüger, and J. Pollmann, Phys. Rev. B **47**, 6971 (1993).
[42] X. W. Zhang, W. J. Fan, S. S. Li, and J. B. Xia, Phys. Rev. B **75**, 205331 (2007).
[43] T. Dietl, J. Phys.: Condens. Matter **19**, 165204 (2007).
[44] P. Sharma, A. Gupta, K. Rao, F. J. Owens, R. Sharma, R. Ahuja, J. M. O. Guillen, B. Johansson, and G. Gehring, Nature Mater. **2**, 673 (2003).
[45] J. F. Cornwell, *Group Theory in Physics* (Academic, London, 1984).